

numerically determine the surface air temperature response function of the atmosphere. Fortunately, this response function has recently been evaluated by three independent experimental means (10). The value obtained over land is 0.175 K per watt per square meter, whereas over the ocean it appears to be at least 50 percent smaller. Thus, for the entire globe, which has 70 percent of its surface area covered by oceans, the mean value of the surface air temperature response function is 0.113 K per watt per square meter or less.

The rise in surface air temperature to be expected from a doubling of the earth's atmospheric CO₂ concentration is consequently determined to be $\leq (0.113 \text{ K W}^{-1} \text{ m}^2) (2.28 \text{ W m}^{-2}) = \leq 0.26 \text{ K}$. For the entire planet, a doubling of the atmospheric CO₂ concentration would produce a change in T_0 practically indistinguishable from climatic "noise," fully an order of magnitude less than the predictions of the theoretical numerical models in vogue today. However, this result is virtually identical to the value of $\leq 0.25 \text{ K}$ obtained by Newell and Dopplick (11). Since these two completely independent experimental studies produce a common result so much lower than previous theoretical estimates, a serious reconsideration of the whole CO₂-climate problem seems imperative.

SHERWOOD B. IDSO
U.S. Water Conservation Laboratory,
4331 East Broadway,
Phoenix, Arizona 85040

References and Notes

1. One possible exception to this consensus is the recent paper by B. Choudhury and G. Kukla [*Nature (London)* 280, 668 (1979)], wherein the authors investigate the effects of increased atmospheric CO₂ on the solar radiation available for absorption by water and snow; the resultant energy deficit, when not compensated by enhanced downwelling atmospheric thermal radiation, may delay the recrystallization of snow and the dissipation of pack ice to yield a cooling rather than a warming effect. Calculations by Newell and Dopplick (11), however, indicate that the thermal radiation enhancement is indeed much larger than the solar radiation reduction, basically negating the possibility raised by Choudhury and Kukla.
2. S. H. Schneider, *J. Atmos. Sci.* 32, 2060 (1975).
3. W. Bach, J. Pankrath, W. Kellogg, Eds., *Man's Impact on Climate* (Elsevier, Amsterdam, 1979).
4. S. Manabe and R. T. Wetherald, *J. Atmos. Sci.* 24, 241 (1967).
5. D. O. Staley and G. M. Jurica, *J. Appl. Meteorol.* 9, 365 (1970); *ibid.* 11, 349 (1972).
6. W. D. Sellers, *Physical Climatology* (Univ. of Chicago Press, Chicago, 1965).
7. S. B. Idso, *J. Atmos. Sci.* 26, 1088 (1969).
8. J. L. Monteith, *Q. J. R. Meteorol. Soc.* 87, 171 (1961).
9. G. W. Paltridge and C. M. R. Platt, *Radiative Processes in Meteorology and Climatology* (Elsevier, Amsterdam, 1976).
10. S. B. Idso, in preparation.
11. R. E. Newell and T. G. Dopplick, *J. Appl. Meteorol.* 18, 822 (1979).
12. Contribution from Agricultural Research, Science and Education Administration, U.S. Department of Agriculture.

1 October 1979; revised 7 January 1980

Core Drilling Through the Ross Ice Shelf (Antarctica) Confirmed Basal Freezing

Abstract. *New techniques that have been used to obtain a continuous ice core through the whole 416-meter thickness of the Ross Ice Shelf at Camp J-9 have demonstrated that the bottom 6 meters of the ice shelf consists of sea ice. The rate of basal freezing that is forming this ice is estimated by different methods to be 2 centimeters of ice per year. The sea ice is composed of large vertical crystals, which form the waffle-like lower boundary of the shelf. A distinct alignment of the crystals throughout the sea ice layer suggests the presence of persistent long-term currents beneath the ice shelf.*

In 1978, as part of the Ross Ice Shelf Project (1), we obtained a core through the ice shelf in the area of Camp J-9 (82° 22'S, 168°37'W; Fig. 1a), using an antifreeze thermal-drilling method. This procedure, developed by V. A. Morev of the Arctic and Antarctic Research Institute, Leningrad, and one us (I.A.Z.), consisted of adding an antifreeze component to the melted water within the hole in order to keep it from freezing at low temperatures, instead of taking this water from the hole. The necessary drilling equipment was designed and built by Morev (2). Core drilling through the ice shelf began on 1 December 1978 (3) and was completed in 13 days. An ethyl alcohol-water solution was used as the antifreeze. Some 416 m of core, with a diameter of about 8 cm, was recovered, including a core from the very bottom of the ice shelf.

The core revealed no debris of any kind throughout the thickness of the ice shelf. The core consists of homogeneous bubbly glacial ice to a depth of 410 m. At this depth, abrupt changes in the appearance and properties of the ice occur. The

6-m-thick lower layer contains vertical brine channels and some brownish material. The salinity of the ice within this layer is much higher than that of the ice above 410 m (Fig. 1b) (4) and increases to the bottom of the ice shelf. These features are typical of ice formed by the freezing of seawater onto the bottom.

Large vertical crystals are observed throughout the 6-m layer. At the bottom of the shelf, the lower ends of these crystals protrude downward into the sea, giving rise to a waffle-like bottom surface (Fig. 2a) (5).

The bottom crystals show distinct alignment at the bottom of the Ross Ice Shelf (shown schematically in Fig. 1c). This alignment can be followed throughout the sea ice layer, showing strong preferred crystal orientation within the layer.

The same kind of alignment, but on a much smaller scale, is found in the growing fast ice of northern polar seas (6, 7). It indicates that there is active freezing at the bottom of the ice shelf at Camp J-9 at the present time. These structure alignments of fast ice were probably formed

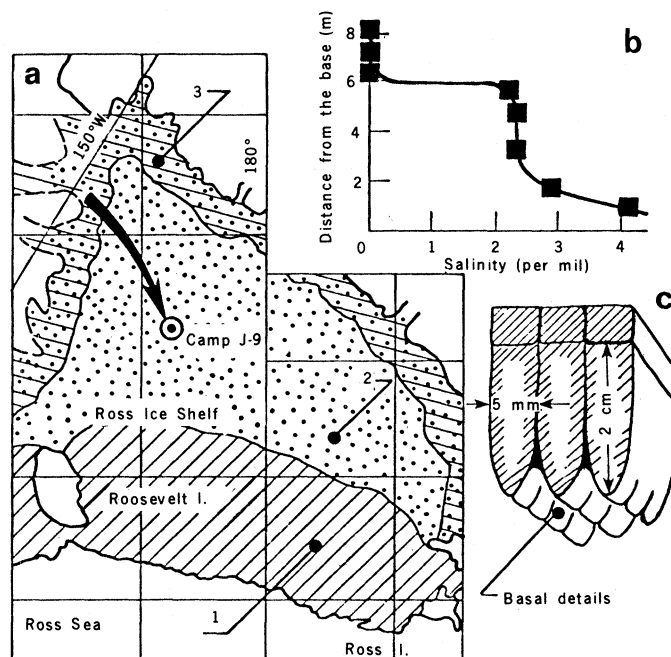


Fig. 1. (a) Map of the Ross Ice Shelf showing the location of Camp J-9 and the approximate stream line of the ice shelf in an area of Camp J-9. Area 1, region of melting at the bottom (δ); area 2, region of freezing governed by heat loss through the ice shelf; area 3, belt of freezing, influenced by a freshwater supply to the bottom of the ice shelf (δ). (b) Salinity of the bottom part of the ice core. (c) Schematic of the crystal alignment at the base of the ice shelf.

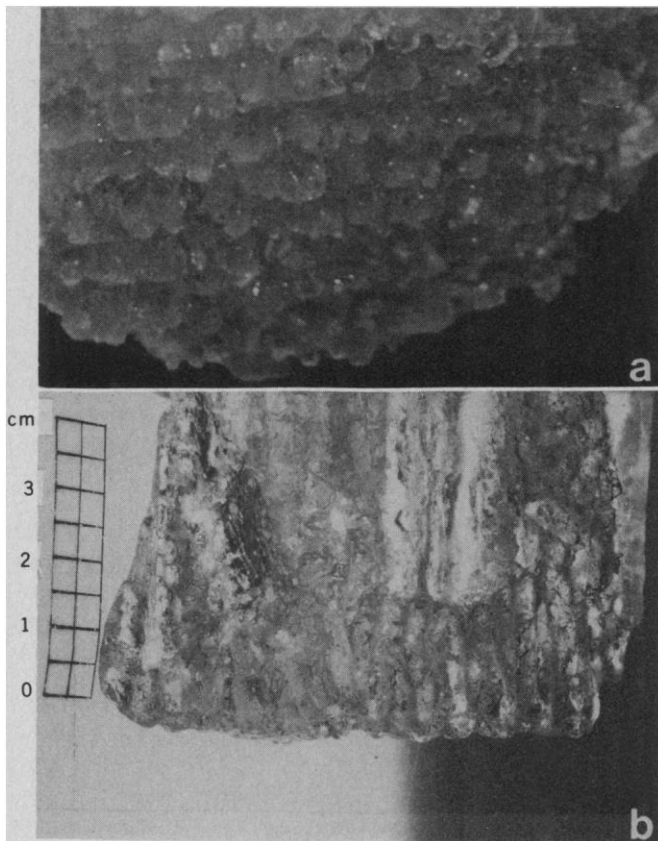


Fig. 2. Photographs of the bottom part of the sea ice layer. (a) Waffle-like bottom of the ice shelf with distinct alignment. (b) Cross section of the bottom part of the ice shelf. The annual layer of ice growth for 1977-78 can be seen.

under the influence of persistent currents, so that the direction of the alignment corresponds to the direction of the currents (7). Because of strong preferred crystal orientation throughout the sea ice layer, this layer can be treated as a very large single crystal, oriented to the direction of the main current below the ice shelf. This feature can thus be used as a remote sensor of current directions below the ice shelf.

The speed of ice growth at the bottom of the Ross Ice Shelf can be determined from a core analysis. The bottom 2 cm of sea ice is distinctly different from the remainder of the 6-m sea ice layer (Fig. 2b). The distinct horizontal boundary separating the bottom 2 cm from the remainder of the sea ice is the only horizontal boundary observed in the 6 m of sea ice. This dramatic change in appearance in the bottom 2 cm indicates a sudden and significant change in growth conditions at the base of the shelf, the most probable cause of which was a penetration of the ice shelf with a flame-jet drill (8) in December 1977 approximately 200 m from the present location of the core hole. If that boundary, 2 cm from the bottom, was the result of the flame-jet drilling 12 months earlier, we infer a present growth rate of 2 cm per year.

The average growth rate for a longer period can be estimated from the overall thickness of the sea layer and the dynam-

ics of the Ross Ice Shelf. The distance from the grounding line to Camp J-9 is about 200 km, and the average ice velocity in this area is 300 to 400 m per year. Thus, the bottom of the J-9 core column has been exposed to seawater for 400 to 600 years and has experienced an average basal ice growth of about 1 to 1.3 cm per year, close to the present annual growth rate at Camp J-9. The upper boundary at this 6-m sea ice layer is porous, slushy ice, a few centimeters thick. When the drilling equipment reached this ice, the level of the water-alcohol solution in the hole rose suddenly to 23 m, where it was in equilibrium with sea level. The porous ice layer thus has a good hydraulic connection with the sea below the layer of solid sea ice.

The possibility of bottom freezing in the rear of the Ross Ice Shelf has been suggested and discussed for many years, but such a phenomenon has also been strongly questioned (9, 10). Recent temperature and salinity profiles (11, 12) in the seawater below the ice shelf at Camp J-9 show a thick, cold isothermal layer of lower salinity in the upper part of the water column, adjacent to the ice-water interface. The temperature in this layer is close to the freezing point.

These data have been interpreted (11) as evidence of bottom melting near Camp J-9. However, the temperature

and salinity profiles would be the same if the water had been cooled to the melting point well before reaching Camp J-9 from the north. Then, in the absence of active heat exchange between the isothermal, cold water layer and the bottom, all the heat produced by freezing would be removed by conduction through the ice shelf. Indeed, temperature measurements within the ice shelf at Camp J-9 show that the heat flux from the water-ice interface is about 120 cal/cm² per year (1). With no heat exchange between the seawater and the ice shelf, the water should be freezing at about 1.6 cm per year at the bottom of the ice shelf.

These results from simple heat-transfer models are in good agreement with the estimates of the ice growth rate obtained from the core analyses. They suggest that there is no strong heat exchange within the seawater column in a horizontal direction and that the seawater temperature profile does not change much along the seawater stream line near Camp J-9.

We can summarize the bottom conditions of the Ross Ice Shelf as follows. A belt of melting exists in the northern part of the Ross Ice Shelf, extending south from the shelf edge for about 200 km (10) (area 1 in Fig. 1a). Active heat exchange becomes less until the heat flow from the water is enough to compensate for heat losses by upward conduction through the ice. Farther south is an area of basal freezing at about 2 cm per year (area 2 in Fig. 1a). Here heat exchange at the ice-water interface is negligible, and freezing is governed by heat loss through the ice sheet. Camp J-9 is located in this zone.

We believe another zone should be designated apart from areas 1 and 2, a zone of freezing that is controlled or initiated by a freshwater supply to the bottom of the ice shelf. This zone is located to the seaward side of the grounding line of the ice shelf (area 3 in Fig. 1a) (10).

IGOR A. ZOTIKOV
VICTOR S. ZAGORODNOV
JURIY V. RAIKOVSKY

*Institute of Geography,
U.S.S.R. Academy of Sciences,
Staromonetny 29,
Moscow 109017, U.S.S.R.*

References and Notes

1. J. W. Clough and B. L. Hansen, *Science* **203**, 433 (1979).
2. V. A. Morev, *Bull. Invent. Discoveries No. 27* (1972); license 350945.
3. Drilling through the ice shelf was sponsored by the National Science Foundation and the U.S.S.R. Academy of Sciences.
4. We thank Dr. Anthony Gow who measured the salinity of water samples from the sea ice layer.
5. The photographs in Fig. 2 were taken at Camp J-9 by Bruce Koscy with the help of Bob De-

- ars, official U.S. Army Cold Regions Research and Engineering Laboratory photographer.
6. N. V. Cherepanov, *Problems Arct.* **38**, 137 (1971).
 7. W. F. Weeks and A. J. Gow, *U.S. Army Cold Regions Res. Eng. Lab. Rep.* 78-13 (1978).
 8. J. A. Browning and D. A. Sommerville, *Antarct. J. U.S.* **13** (No. 4), 55 (1978).
 9. J. H. Zumberge, *Antarct. Res. Ser.* **2**, 65 (1964); M. B. Giovinetto and J. H. Zumberge, *Int. Assoc. Sci. Hydrol. Publ.* **79** (1968), p. 255; A. L. Gordon, *Antarct. J. U.S.* **4** (No. 5), 183 (1969); S. S. Jacobs, F. M. Amos, P. M. Bruchhausen, *Deep-Sea Res.* **17**, 935 (1970); I. A. Zotikov, in *Colloque d'Oberqurgl* (International Association of Scientific Hydrology, Paris, 1963), pp. 36-49.
 10. I. A. Zotikov, thesis, Institute of Geography, U.S.S.R. Academy of Sciences (1970); *Gidrometeorizdat* (Hidrometeorological Publishing House, Leningrad, 1977) (on pp. 141-146, Zotikov introduces a model of freezing under the influence of a freshwater supply to the bottom of the ice shelf; figure 50 shows a map of the freezing area at the base).
 11. A. E. Gilmour, *Science* **203**, 438 (1979); S. S. Jacobs, A. L. Gordon, J. L. Ardal, Jr., *ibid.*, p. 439.
 12. T. D. Foster, *Antarct. J. U.S.* **13** (No. 4), (1978).
 13. The first draft was written by I.A.Z. while he was a visiting scientist at the U.S. Army Cold Regions Research and Engineering Laboratory, Hanover, N.H. We thank the personnel of the U.S. Antarctic Program; the Ross Ice Shelf Project, especially W. Reirden, I. Virschieks, M. Wolf, and U. Auderes who took part in drilling through the ice shelf; the U.S. Army Cold Regions Research and Engineering Laboratory; and the National Science Foundation for assistance and cooperation.

25 June 1979; revised 23 October 1979

Geothermal System at 21°N, East Pacific Rise: Physical Limits on Geothermal Fluid and Role of Adiabatic Expansion

Abstract. Pressure-volume-temperature relations for water at the depth of the magma chamber at 21°N on the East Pacific Rise suggest that the maximum subsurface temperature of the geothermal fluid is about 420°C. Both the chemistry of the discharging fluid and thermal balance considerations indicate that the effective water/rock ratios in the geothermal system are between 7 and 16. Such low ratios preclude effective metal transport at temperatures below 350°C, but metal solubilization at 400°C and above is effective even at such low ratios. It is proposed that the 420°C fluid ascends essentially adiabatically and in the process expands, cools, and precipitates metal sulfides within the upper few hundred meters of the sea floor and on the sea floor itself.

The discoveries by manned submersible of actively forming massive sulfide deposits at 21°N on the East Pacific Rise (1, 2) substantiate the long-held belief that such deposits are associated with sea-floor spreading. The discharging fluids are apparently actively precipitating a deposit largely composed

of sphalerite, chalcopyrite, anhydrite, and barite (3, 4).

The temperature of the fluid is unexpectedly high (2), and a reevaluation of the conditions of fluid generation is warranted. The purpose of this report is to consider the possible pressure and temperature limits on the fluid in the sub-

surface and the implications these limits might have for the mechanisms of metal transport and deposition.

It has been commonly held that connecting seawater cools the upper portion of new oceanic crust and in the process alters the rocks and leaches heavy metals at maximum temperatures of about 350°C. Mineral deposition was believed to result from cooling of this fluid.

This model does not easily apply to the system at 21°N. Experimental studies have shown that during cooling of heated seawater, silica should overwhelmingly dominate the precipitation products (5), yet silica is a relatively minor component of the observed assemblage at 21°N (3, 4). Moreover, adequate concentrations of heavy metals are solubilized at 350°C only when water/rock ratios during inter-action are large (6), whereas experimental results show that the water/rock ratio does not control metal solubilization above about 400°C (7).

An estimated exit temperature of $390 \pm 10^\circ\text{C}$ was reported for a single vent by Speiss *et al.* (2) from dives carried out with the submersible *Alvin* during the spring of 1979 at 21°N. During the dives in the fall of 1979 the temperature directly observed at several vents was 350°C (8), suggesting that the earlier estimate might be spurious. However, later examination of the chart record of *Alvin's* temperature probe indicated two measurements during the final dive in excess of 400°C (9). During the fall 1979 dives samples of the hydrothermal fluid were taken but were contaminated by various amounts of seawater. Plots of

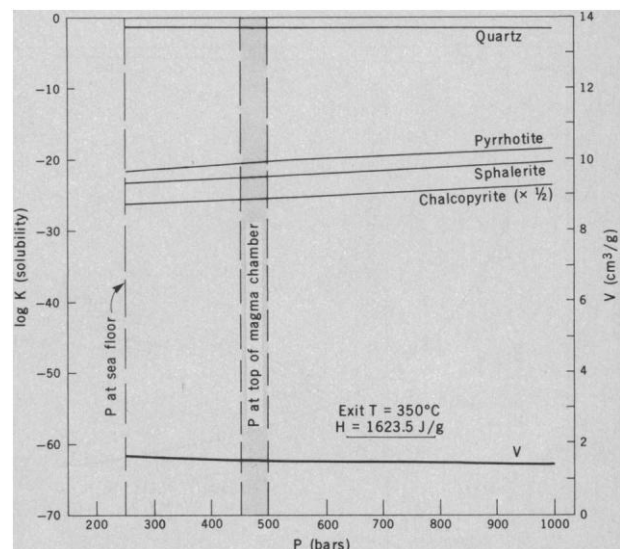
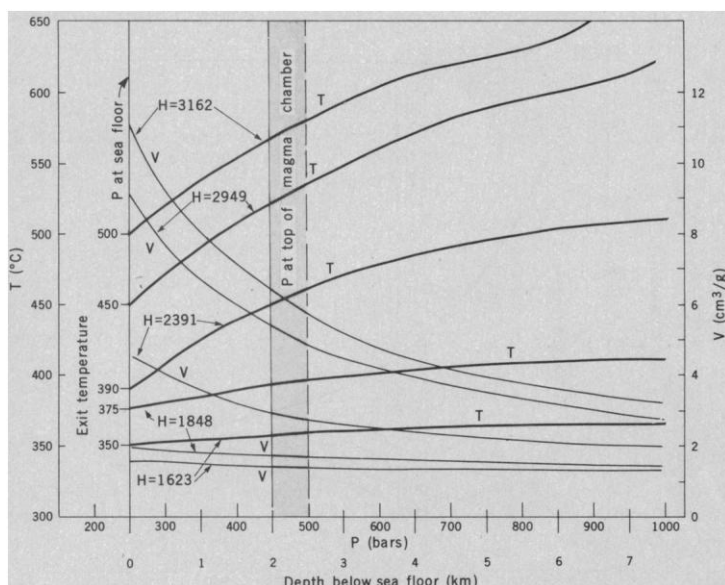


Fig. 1 (left). Changes in water temperature T and specific volume V as a function of pressure at constant enthalpy H (adiabatic compression). Relations calculated from data in (27) for sea-floor exit temperatures of 350°, 375°, 390°, 450°, and 500°C. Fig. 2 (right). Solubility constants of minerals and specific volume of water as a function of pressure at a constant enthalpy (adiabatic) of 1623 J/g, corresponding to a sea-floor exit temperature of 350°C. In Figs. 2 through 6, data for water volume are from (27) and solubility constants were calculated by SUPCRT (17).